Journal of Materials Chemistry C

Accepted Manuscript

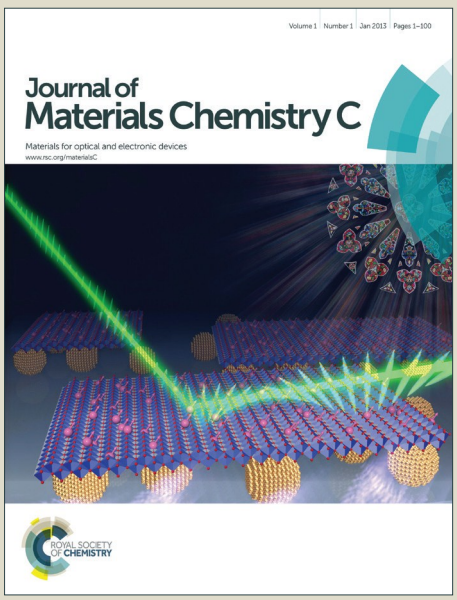

ROYAL SOCIETY OF CHEMISTRY

www.rsc.org/materialsC

Patterning of rubrene thin-film transistors based on electron irradiation of a polystyrene dielectric layer

Jae Joon Kim [a], Hyeok Moo Lee [b], Ji Won Park [a], and Sung Oh Cho [a]

[a] Jae Joon Kim, Ji Won Park and Sung Oh Cho: Department of Nuclear and Quantum Engineering, Korea Advanced Institute of Science and Technology, Daejeon 305-701 (Korea)

[b] Hyeok Moo Lee: Informative Electronic Materials Lab., LG Chemistry Research Park, Daejeon 305-738 (Korea)

Abstract

An unprecedented approach to fabricate patterned rubrene thin-film transistors (TFTs) is presented by combining an abrupt heating method with selective electron irradiation of polystyrene dielectric layers. We found that an amorphous rubrene is crystallized only on electron-irradiated polystyrene (PS) while no crystallization of rubrene occurs on unirradiated PS by the abrupt heating process. Based on this finding, patterned rubrene semiconductor could be successfully fabricated by irradiating an electron beam onto selective regions of a PS layer followed by the abrupt heating process. The patterned rubrene TFTs exhibited good performances with charge mobilities of ~1.3 $cm^2V^{-1}s^{-1}$ and on/off ratios higher than 10^8.

Introduction

Organic thin-film transistors (OTFTs) have attracted great attention of researchers due to the applications to flexible displays,[1] bio-compatible sensors,[2] and low-cost electronics like radio frequency identification tags.[3] For these applications, proper selection of an organic semiconductor material is crucial. Though several organic semiconductor materials showed good performances in charge carrier mobility, other requirements such as high stability and low cost should also be satisfied for the practical applications of the OTFT devices.[4] In this respect, rubrene is one of the best organic semiconductor materials due to the following features. First, single-crystalline rubrene exhibited very high charge mobility up to 20 $cm^2V^{-1}s^{-1}$.[5] Second, rubrene is highly soluble in common solvents such as toluene, and does not need toxic chlorinated solvents or functionalization of molecules.[6] Last, pure sublimed rubrene is commercialized with a competitive price compared to other organic semiconductors. However, for the applications to organic electronics, thin-filmed semiconductor materials are necessary, but simple and reliable methods to prepare high-quality crystalline rubrene thin films are still challenging.

We recently demonstrated a simple, so called, 'abrupt heating method' to fabricate crystalline rubrene thin films.[7, 8] Well-ordered, high-crystalline orthorhombic rubrene thin films are created through the abrupt heating method, which crystallizes amorphous rubrene films on a substrate by increasing the annealing temperature very rapidly in ambient air. OTFTs made of the rubrene thin films showed charge mobilities higher than 1 $cm^2V^{-1}s^{-1}$ on a bare SiO_2 substrate.[7]

Meanwhile, patterning of an organic semiconductor is required to improve the performance of an OTFT, particularly, on/off ratio of the device. Unwanted crosstalk and gate leakage current are significantly decreased via patterning, which leads to a dramatic decrease in the off current while maintaining the on current level.[9] Mainly, two different patterning methods have been developed: a selective removal method and a selective deposition method. In a selective removal method, a crystalline organic semiconductor film is prepared on a dielectric followed by the removal of unwanted area of the semiconductor layer by top-down approaches including reactive ion etching,[10] soft

lithography,[11] and electron or UV lithography.[12] However, the semiconductor films can be damaged or contaminated during the removal process, which can affect the performance of the OTFTs negatively. These problems can be overcome through a selective deposition method, where organic semiconducting molecules are directly deposited only on selected region of dielectrics. In case of pre-treatment, dielectric layer is treated prior to the deposition of semiconducting layer with functional materials such as self-assembled monolayers[13] or fluoropolymer.[14] Due to the difference in the surface energies between the treated and non-treated dielectric regions, the semiconducting molecules are attached only to the treated or non-treated dielectric surface. However, since this technique relies on the self-assembly of vapor- or solution-based separate organic molecules, the pre-defined dielectric layer tend not to be uniformly and completely covered with semiconducting molecules. Hence, the fabricated semiconductor thin film comprises uneven crystallites. Furthermore, the organic molecules can be attached to undesired regions, resulting in non-uniform and irregular semiconductor patterns with unclear boundaries.[15] In addition, organic semiconducting materials can also be selectively deposited by printing methods. Large-area and patterned organic semiconducting layer can be formed through this one-step fabrication method.[16] However, the spatial resolution of the pattern is limited due to the finite size of nozzle. Also, the patterned area of semiconductor tends to have very rough surface and irregular crystalline structure.[17] Consequently, the devices based on these selective deposition methods show poor performances with large variations.

Here, we present an unprecedented approach to fabricate patterned rubrene TFTs by combining our abrupt heating method with selective electron irradiation of PS dielectric layer. The patterned rubrene TFTs fabricated by the approach exhibited good performances with an average charge mobility of 1.3 $cm^2V^{-1}s^{-1}$ and an average on/off ratio higher than 10^8.

Results and discussion

The procedure to fabricate patterned rubrene TFTs is illustrated in Fig. 1. First, a PS layer is spin-coated on a SiO_2/Si substrate and then is irradiated with an electron beam through a metal mask.

Electron irradiation directly induces crosslinking of PS molecular chains without any chemical agents, and thus, only the electron-irradiated regions of the PS layer are crosslinked. Subsequently, amorphous rubrene is deposited on the PS layer via thermal evaporation. The as-deposited rubrene film is abruptly heated by placing the sample on a preheated hot plate in ambient conditions. This abrupt heating process leads to the crystallization of rubrene only on crosslinked PS while rubrene on non-crosslinked PS keeps its original amorphous phase. As a consequence, patterned crystalline rubrene thin films are fabricated. Two gold electrodes are then thermally evaporated on each rubrene semiconductor pattern, resulting in patterned rubrene TFTs.

Fig. 2 shows the polarized optical microscope (POM) and atomic force microscope (AFM) images of the crystalline rubrene thin films fabricated on PS layers that were electron-irradiated at different fluences. The rubrene films were crystallized through the abrupt heating process at 170 ^{0}C, which was the optimum temperature for the crystallization of the rubrene films (Fig. S1). When a rubrene film on unirradiated PS was abruptly heated, no crystallization occurred (Fig. 2a). However, as the electron fluence was increased, the crystallinity of a rubrene film was gradually improved. When the electron fluence was increased to 1×10^{16} cm^{-2}, many rubrene crystals with a triclinic phase were formed (Fig. 2b): line-shaped morphologies in the POM and AFM images reflect a triclinic phase of rubrene.[7] The rubrene crystalline domains became more regular when the electron fluence was increased to 5×10^{16} cm^{-2}, but triclinic phase of rubrene still existed and the crystalline domains had slightly curved boundaries (Fig. 2c). In contrast, well-faceted and interconnected rubrene films, suggesting the orthorhombic phase of rubrene crystals,[7] were created over the whole PS surface at the electron fluence of 2×10^{17} cm^{-2} (Fig. 2d). No color variation was observed within a single domain under the POM investigation, indicating that a domain was composed of a single crystal.[7, 8] The average domain size was as high as 50 μm.

The effects of electron irradiation on the crystallization of rubrene thin films can be explained as follows. If an amorphous rubrene film on an unirradiated PS layer is abruptly heated at the optimum temperature of 170 ^{0}C, the molecular chains of the underlying PS can actively and randomly move. This

is because the annealing temperature is much higher than the glass transition temperature (ca. 100 °C) of PS. The randomly moving PS chains disturb the regular ordering of overlying rubrene molecules,[18] and hence, a rubrene film on unirradiated PS can hardly be crystallized by the abrupt heating process (Fig. 2a). However, if PS is electron-irradiated, the PS chains cannot easily move because the molecular chains of PS are three-dimensionally crosslinked by the irradiation.[19] As a result, when an amorphous rubrene film on an electron-irradiated PS layer is abruptly heated at 170 ^{0}C, the rubrene molecules can be thermally rearranged to form crystals without a disturbance of underlying PS and accordingly a crystalline rubrene film is created on the PS layer. The quality of the crystalline rubrene film or the degree of crystallinity is determined by the crosslinking ratio of PS. Since the crosslinking ratio is increased with the increase in the electron fluence (Fig. 2e), a rubrene film with better crystallinity is produced on electron-irradiated PS as the electron fluence was increased (Fig. 2a-d). This fact was confirmed by the electrical characteristics of OTFTs made of the rubrene thin films. As shown in Fig. 2f, an amorphous rubrene film formed on unirradiated PS exhibited a very low charge mobility of ~10^{-3} $cm^2V^{-1}s^{-1}$. However, the charge mobilities of the rubrene TFTs on irradiated PS increased as the electron fluence was increased. The mobility value reached up to 1.25 $cm^2V^{-1}s^{-1}$ when the electron fluence was above 2×10^{17} cm^{-2}.

In addition, two-dimensional grazing incidence X-ray diffraction (GIXD) pattern of the crystalline rubrene thin film displayed many strong and sharp reflection spots (Fig. 3a). It clearly reveals that the rubrene film consists of highly-ordered orthorhombic crystals and that the *ab* planes of the crystals are perfectly oriented parallel to the substrate surface while *c* axes of the crystals are aligned perpendicular to the substrate. X-ray diffraction (XRD) patterns of the rubrene films (Fig. 3b) also show a diffraction peak at $2\theta = 6.54^0$, corresponding to (002) plane of orthorhombic rubrene crystal.[20] The XRD peak intensity of the rubrene film formed on electron-irradiated PS is higher than that formed on SiO_2, suggesting that a rubrene film with better crystallinity is formed on electron-irradiated PS than on SiO_2. The performances of OTFTs also confirm this fact: the average mobility (1.25 $cm^2V^{-1}s^{-1}$) of the rubrene TFTs on electron-irradiated PS was higher than that (1.03 $cm^2V^{-1}s^{-1}$) of the rubrene TFTs on SiO_2

fabricated at the same experimental conditions. To analyze the reasons of the improvements in both the crystallinities and charge mobilities of the rubrene films on electron-irradiated PS compared to SiO_2, the interfaces between rubrene films and dielectric layers were investigated. First, the surface roughness (R_q) of the PS layer irradiated at the electron fluence of 2×10^{17} was 0.19 nm, which is almost comparable to that of SiO_2 (R_q = 0.20 nm). However, the surface energy (26.3 mJ/m^2) of the electron-irradiated PS layer is much lower than that (54.11 mJ/m^2) of SiO_2 (Table 1). In terms of the surface energy, the crystalline rubrene having the surface energy of 33.9 mJ/m^2 is more well-matched to electron-irradiated PS than to SiO_2. Due to the relatively well-matching of the surface energies at the interface, both the crystallinity and the charge mobility of the rubrene film were enhanced on electron-irradiated PS than SiO_2.[21]

In addition, the fact that crystalline rubrene films are formed only on electron-irradiated PS provides us a novel strategy to fabricate patterned rubrene crystal films. If selected regions of a PS layer are electron-irradiated followed by abrupt heating of an amorphous rubrene film as shown in Fig. 1, rubrene only on irradiated regions of PS is crystallized while amorphous rubrene is left on unirradiated regions of PS. This strategy was demonstrated in Fig. 4 where a metal mask with rectangular holes was used for the selective electron irradiation on a PS layer. The POM images show that continuously interconnected orthorhombic rubrene crystals were formed only inside each rectangular pattern that was electron-irradiated (Fig. 4a, b). No crystals were formed at the outside of the rectangles that were not electron-irradiated, even though the outside regions were also covered with amorphous rubrene. Consequently, the rectangular patterns had very clear boundaries of crystals between the irradiated and unirradiated regions (inset of Fig. 4b). Additionally, the crystalline rubrene thin film in the pattern had a very smooth surface: the measured surface roughness of the rubrene film was ~1 nm. This smooth surface is desirable for OTFT applications because metal electrodes can be well attached to the rubrene semiconductor, and hence, contact resistance between the electrodes and the organic semiconductor can be reduced.[22]

One thing to note here is that the thickness of a PS layer affects the morphology of the crystalline rubrene pattern. When a PS layer thickness was too small (≤ 10 nm), rubrene crystals were sparsely formed even on unirradiated PS regions in addition to irradiated regions, leading to the formation of an unclear crystalline rubrene pattern (Fig. S2a). This is because the movement of polymer chains in a very thin PS layer is not sufficiently active to hinder the crystallization of rubrene molecules on unirradiated PS. In order to get clear crystalline rubrene patterns, enough thick PS layers were required (Fig. S2b, c, d). However, a large thickness of the PS dielectric layer increases the operating voltage and decreases the on current of OTFT devices (Fig. S3). After the systematic experiments and analyses, we observed that the optimum PS thickness was ~20 nm at which both a clear pattern of the crystalline rubrene film and a good OTFT performance were achieved.

After the successful formation of the patterned rubrene thin films, two gold electrodes were deposited on the rubrene semiconductor film in each rectangular pattern, thereby resulting in patterned OTFTs (Fig. 4c). Operational characteristics of both patterned rubrene TFTs and unpatterned rubrene TFTs were shown in Fig. 5. The average charge mobility of the patterned rubrene TFTs was 1.30 $cm^2V^{-1}s^{-1}$ while that of unpatterned rubrene TFTs was 1.25 $cm^2V^{-1}s^{-1}$, indicating that the mobilities of the rubrene TFTs were almost unchanged after the patterning. However, the gate leakage current was dramatically decreased after the patterning. The maximum leakage current of the patterned device was about four orders lower than that of the unpatterned device. The off current of the patterned rubrene TFT was also drastically decreased compared to the unpatterned rubrene TFTs. Consequently, the average on/off ratio of the OTFTs was increased from 5×10^4 to 1×10^8 after the patterning.

One more thing to note here is that PS molecular chains can also be crosslinked by UV irradiation as well as electron irradiation.[23] Therefore, we could successfully produce patterned crystalline rubrene thin films by combining UV irradiation with the abrupt heating process (Fig. S4). The crystalline rubrene thin films made by UV irradiation have almost the same morphologies with those made by electron irradiation.

Experimental

Sample Fabrication

PS layers were prepared by spin coating of PS (Sigma Aldrich, Mw = 2,000,000 g/mol) dissolved in toluene on a 100 nm SiO2 gate dielectric underlying heavily doped n-type silicon substrate. Subsequently, the samples were irradiated with a 30 keV electron beam generated by a home-made thermionic electron gun under vacuum (a pressure less than 10^{-5} torr). After the electron irradiation, the samples were rinsed in isopropyl alcohol and dried under nitrogen follow. Amorphous rubrene film with the thickness of ~20 nm was then deposited by a thermal evaporation of rubrene powders (sublimed grade, Sigma-Aldrich, Inc.). The abrupt heating process was carried out by placing a sample onto a hot plate pre-heated at 170 °C in ambient conditions and in a dark room. The heating process lasted for 90 s. Au electrodes with the thickness of 100 nm were evaporated by a mask for the fabrication of OTFTs. The OTFTs have the channel widths of 1000 μm and the channel length of 50 μm. Also, UV-induced crosslinking of PS was performed using UV light (wavelength is 254 nm) of UV lamp (EEC, VL-4.LC).

Measurements

POM images were captured using an optical microscope (Olympus, BX51) and the topographies were examined with an AFM (Park Systems, XE-70). The crosslinking ratio of irradiated PS was measured using gel permeation chromatography (Waters, Aliance 2690). The contact angle was measured by placing 3 μL droplet of a solution onto a flat sample surface. The crystalline structures of the rubrene films were characterized with XRD (RIGAKU, D/MAX-2500) and GIXD measurements using the 4C2 beamline at the Pohang Accelerator Laboratory. The diffraction patterns were recorded using a MarCCD detector. The grazing-incidence angle of the X-ray beam (λ = 1.3807 Å) was varied between 0.140 and 0.250. The diffraction data were displayed as an intensity map in which q_{xy} is the in-plane momentum transfer and q_z is the out-of-plane momentum transfer. The OTFT characteristics were evaluated using a probe station (Semiconductor Characterization System 4200 SCS/F and Summit 11862B, Keithley and Cascade) in ambient conditions. The average mobility and on/off ratio of the OTFTs were achieved by measuring the electrical characteristics of at least 5 devices.

Conclusion

In summary, we have presented an unconventional approach to fabricate patterned rubrene TFTs based on the fact that amorphous rubrene is crystallized on electron-irradiated PS while no crystallization of rubrene occurs on unirradiated PS by the abrupt heating process. The patterning approach has a few advantages. First, the rubrene semiconductor pattern has clear boundaries between the electron-irradiated and unirradiated regions, thereby allowing well-defined organic semiconductor pattern structures. Second, the rubrene semiconductor thin films produced in the pattern comprise well-interconnected and high-quality crystalline rubrene. Third, the crystalline rubrene thin films with very uniform and smooth surfaces are created in the pattern. Consequently, the patterned OTFTs fabricated by the approach exhibited good device performances with high charge mobilities and high on/off ratios. Therefore, we believe that the present approach can provide a useful way to expedite the practical applications of rubrene TFTs to various organic electronics.

Acknowledgement

This work was supported by the basic research program of the Korea Atomic Energy Research Institute (KAERI) Grant funded by the Korea government (N04130036).

Notes

Electronic Supplementary Information (ESI) available: POM images of crystalline rubrene thin films abruptly heated at different conditions, GIXD pattern and XRD spectra of crystalline rubrene thin films, POM images of rubrene thin-film patterns fabricated on PS layers with different thickness, transfer characteristics of rubrene TFTs with different thickness, and POM image of patterned crystalline rubrene thin-film on UV-irradiated PS. See DOI: 10.1039/b000000x/

References

1. G. H. Gelinck, H. E. Huitema, E. van Veenendaal, E. Cantatore, L. Schrijnemakers, J. B. van der Putten, T. C. Geuns, M. Beenhakkers, J. B. Giesbers, B. H. Huisman, E. J. Meijer, E. M. Benito, F. J. Touwslager, A. W. Marsman, B. J. van Rens and D. M. de Leeuw, *Nat. Mater.*, 2004, **3**, 106; J. A. Rogers and Z. Bao, *J. Polym. Sci., Part A: Polym. Chem.*, 2002, **40**, 3327.
2. L. Li, P. Gao, M. Baumgarten, K. Mullen, N. Lu, H. Fuchs and L. Chi, *Adv. Mater.*, 2013, **25**, 3419; C. Liao and F. Yan, *Polymer Reviews*, 2013, **53**, 352; T. Sekitani, T. Yokota, U. Zschieschang, H. Klauk, S. Bauer, K. Takeuchi, M. Takamiya, T. Sakurai and T. Someya, *Science*, 2009, **326**, 1516.
3. P. F. Baude, D. A. Ender, M. A. Haase, T. W. Kelley, D. V. Muyres and S. D. Theiss, *Appl. Phys. Lett.*, 2003, **82**, 3964; V. Subramanian, J. M. J. Frechet, P. C. Chang, D. C. Huang, J. B. Lee, S. E. Molesa, A. R. Murphy, D. R. Redinger and S. K. Volkman, *Proc. IEEE*, 2005, **93**, 1330.
4. Z. Bao, *Adv. Mater.*, 2000, **12**, 227; J. Mei, Y. Diao, A. L. Appleton, L. Fang and Z. Bao, *J. Am. Chem. Soc.*, 2013, **135**, 6724.
5. V. C. Sundar, J. Zaumseil, V. Podzorov, E. Menard, R. L. Willett, T. Someya, M. E. Gershenson and J. A. Rogers, *Science*, 2004, **303**, 1644; J. Takeya, M. Yamagishi, Y. Tominari, R. Hirahara, Y. Nakazawa, T. Nishikawa, T. Kawase, T. Shimoda and S. Ogawa, *Appl. Phys. Lett.*, 2007, **90**, 102120.
6. T. Matsukawa, Y. Takahashi, T. Tokiyama, K. Sasai, Y. Murai, N. Hirota, Y. Tominari, N. Mino, M. Yoshimura, M. Abe, J. Takeya, Y. Kitaoka, Y. Mori, S. Morita and T. Sasaki, *Jpn. J. Appl. Phys.*, 2008, **47**, 8950; N. Stingelin-Stutzmann, E. Smits, H. Wondergem, C. Tanase, P. Blom, P. Smith and D. de Leeuw, *Nat. Mater.*, 2005, **4**, 601.
7. H. M. Lee, H. Moon, H.-S. Kim, Y. N. Kim, S.-M. Choi, S. Yoo and S. O. Cho, *Org. Electron.*, 2011, **12**, 1446.
8. H. M. Lee, J. J. Kim, J. H. Choi and S. O. Cho, *ACS Nano*, 2011, **5**, 8352.

9. I. Kymissis, C. D. Dimitrakopoulos and S. Purushothaman, *J. Vac. Sci. Technol. B*, 2002, **20**, 956; S. Liu, H. A. Becerril, M. C. LeMieux, W. M. Wang, J. H. Oh and Z. Bao, *Adv. Mater.*, 2009, **21**, 1266.

10. S. Steudel, K. Myny, S. De Vusser, J. Genoe and P. Heremans, *Appl. Phys. Lett.*, 2006, **89**, 183503.

11. Z. Wang, J. Zhang, R. Xing, J. Yuan, D. Yan and Y. Han, *J. Am. Chem. Soc.*, 2003, **125**, 15278; M. Ofuji, A. J. Lovinger, C. Kloc, T. Siegrist, A. J. Maliakal and H. E. Katz, *Chem. Mater.*, 2005, **17**, 5748.

12. B. A. Mattis, Y. Pei and V. Subramanian, *Appl. Phys. Lett.*, 2005, **86**, 033113; C. Balocco, L. A. Majewski and A. M. Song, *Org. Electron.*, 2006, **7**, 500.

13. A. L. Briseno, S. C. Mannsfeld, M. M. Ling, S. Liu, R. J. Tseng, C. Reese, M. E. Roberts, Y. Yang, F. Wudl and Z. Bao, *Nature*, 2006, **444**, 913; K.-J. Chang, F.-Y. Yang, C.-C. Liu, M.-Y. Hsu, T.-C. Liao and H.-C. Cheng, *Org. Electron.*, 2009, **10**, 815; Y. Li, C. Liu, A. Kumatani, P. Darmawan, T. Minari and K. Tsukagoshi, *AIP Advances*, 2011, **1**, 022149; T. Minari, M. Kano, T. Miyadera, S.-D. Wang, Y. Aoyagi and K. Tsukagoshi, *Appl. Phys. Lett.*, 2009, **94**, 093307.

14. Y. Fujisaki, H. Ito, Y. Nakajima, M. Nakata, H. Tsuji, T. Yamamoto, H. Furue, T. Kurita and N. Shimidzu, *Appl. Phys. Lett.*, 2013, **102**, 153305; S. H. Kim, D. Choi, D. S. Chung, C. Yang, J. Jang, C. E. Park and S.-H. K. Park, *Appl. Phys. Lett.*, 2008, **93**, 113306; Y. Li, C. Liu, Y. Xu, T. Minari, P. Darmawan and K. Tsukagoshi, *Org. Electron.*, 2012, **13**, 815.

15. H. S. Lee, D. Kwak, W. H. Lee, J. H. Cho and K. Cho, *The Journal of Physical Chemistry C*, 2010, **114**, 2329; Y. Li, C. Liu, A. Kumatani, P. Darmawan, T. Minari and K. Tsukagoshi, *Org. Electron.*, 2012, **13**, 264; C. Liu, Y. Li, M. V. Lee, A. Kumatani and K. Tsukagoshi, *Phys. Chem. Chem. Phys.*, 2013, **15**, 7917; K. Masataka, M. Takeo and T. Kazuhito, *Applied Physics Express*, 2010, **3**, 051601.

16. N. A. Azarova, J. W. Owen, C. A. McLellan, M. A. Grimminger, E. K. Chapman, J. E. Anthony and O. D. Jurchescu, *Org. Electron.*, 2010, **11**, 1960; K. Fukuda, Y. Takeda, Y. Yoshimura, R.

Shiwaku, L. T. Tran, T. Sekine, M. Mizukami, D. Kumaki and S. Tokito, *Nat Commun*, 2014, **5**, 4147; H. Minemawari, T. Yamada, H. Matsui, J. Tsutsumi, S. Haas, R. Chiba, R. Kumai and T. Hasegawa, *Nature*, 2011, **475**, 364; C. Yun, J. Choi, H. W. Kang, M. Kim, H. Moon, H. J. Sung and S. Yoo, *Adv. Mater.*, 2012, **24**, 2857.

17. K. Hwang do, R. R. Dasari, M. Fenoll, V. Alain-Rizzo, A. Dindar, J. W. Shim, N. Deb, C. Fuentes-Hernandez, S. Barlow, D. G. Bucknall, P. Audebert, S. R. Marder and B. Kippelen, *Adv. Mater.*, 2012, **24**, 4445; B. Kang, W. H. Lee and K. Cho, *ACS applied materials & interfaces*, 2013, **5**, 2302; Y. Wen, Y. Liu, Y. Guo, G. Yu and W. Hu, *Chem. Rev.*, 2011, **111**, 3358.

18. M. Jang, K. Y. Baek and H. Yang, *The Journal of Physical Chemistry C*, 2013, **117**, 25290.

19. J. J. Kim, Y. Li, E. J. Lee and S. O. Cho, *Langmuir*, 2011, **27**, 2334; Y. Li, E. J. Lee, W. Cai, K. Y. Kim and S. O. Cho, *ACS Nano*, 2008, **2**, 1108; H. M. Lee, Y. N. Kim, B. H. Kim, S. O. Kim and S. O. Cho, *Adv. Mater.*, 2008, **20**, 2094.

20. E. Menard, A. Marchenko, V. Podzorov, M. E. Gershenson, D. Fichou and J. A. Rogers, *Adv. Mater.*, 2006, **18**, 1552.

21. J. Gao, K. Asadi, J. B. Xu and J. An, *Appl. Phys. Lett.*, 2009, **94**, 093302; J. Kim, S. H. Kim, T. K. An, S. Park and C. E. Park, *Journal of Materials Chemistry C*, 2013, **1**, 1272; H. S. Lee, K. Park, J.-D. Kim, T. Han, K. H. Ryu, H. S. Lim, D. R. Lee, Y.-J. Kwark and J. H. Cho, *J. Mater. Chem.*, 2011, **21**, 6968; X. Sun, C.-a. Di and Y. Liu, *J. Mater. Chem.*, 2010, **20**, 2599.

22. A. Petrović, E. Pavlica, G. Bratina, A. Carpentiero and M. Tormen, *Synth. Met.*, 2009, **159**, 1210; D. J. Gundlach, L. Zhou, J. A. Nichols, T. N. Jackson, P. V. Necliudov and M. S. Shur, *J. Appl. Phys.*, 2006, **100**, 024509; X. Gao, W. Wu, Y. Liu, S. Jiao, W. Qiu, G. Yu, L. Wang and D. Zhu, *J. Mater. Chem.*, 2007, **17**, 736.

23. M. Yan and B. Harnish, *Adv. Mater.*, 2003, **15**, 244.

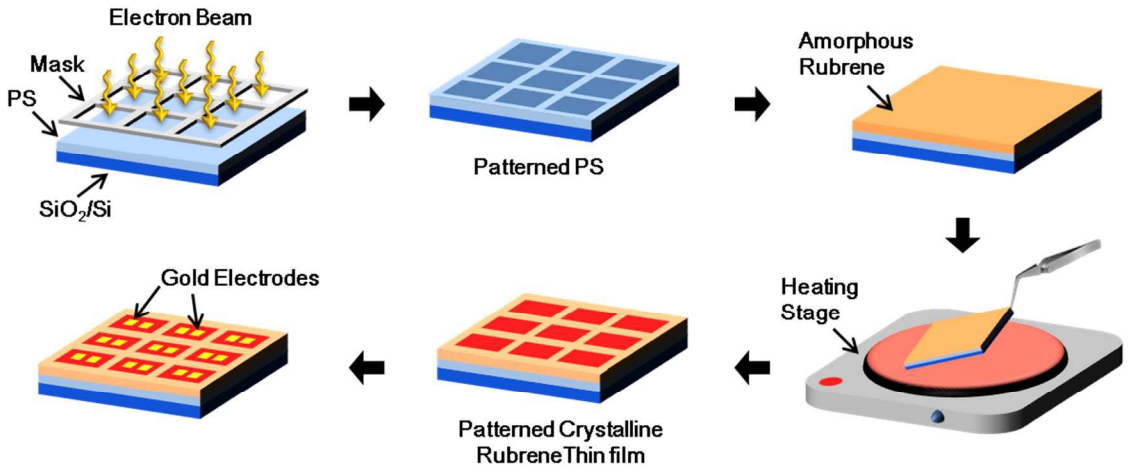

Fig. 1. A schematic illustration to show the fabrication process of patterned rubrene TFTs.

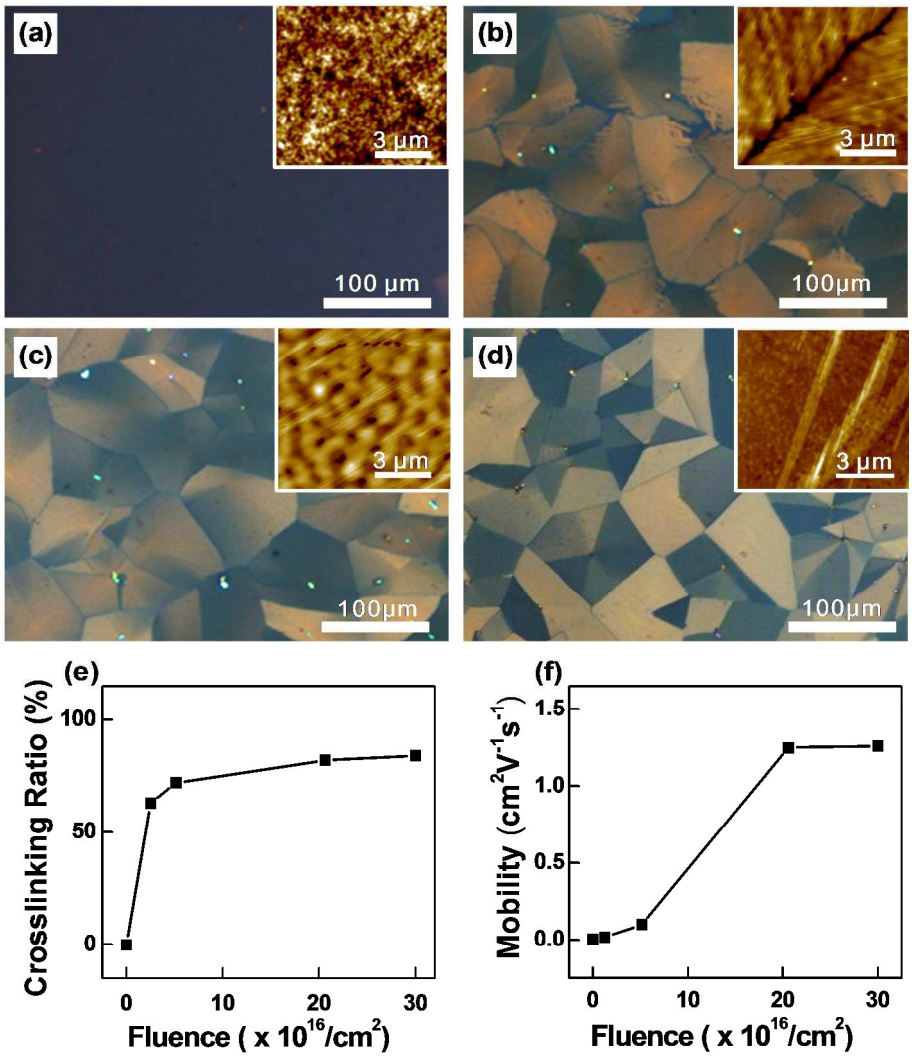

Fig. 2. (a-d) POM images of crystalline rubrene thin films prepared on PS layers that are electron-irradiated at different fluences; (a) 0 cm^{-2}, (b) 1×10^{16} cm^{-2}, (c) 5×10^{16} cm^{-2}, and (d) 2×10^{17} cm^{-2}. The insets are AFM images of the corresponding samples. (e) Crosslinking ratio of PS and (f) charge mobilities of rubrene TFTs prepared on irradiated PS as a function of electron fluence.

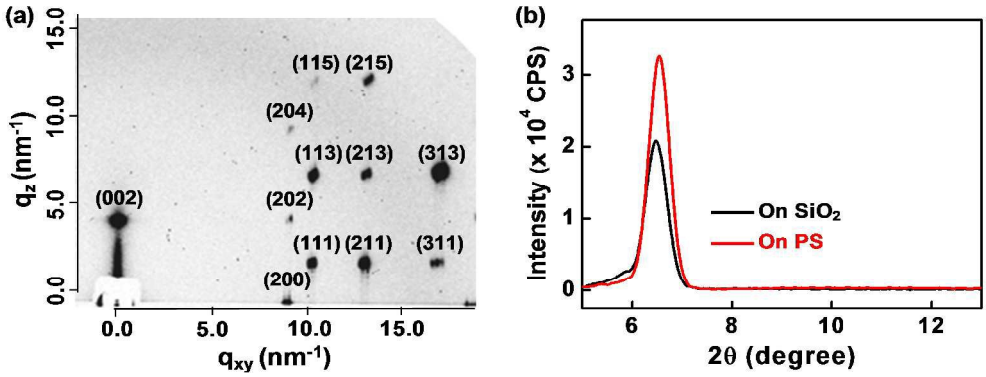

Fig. 3. (a) GIXD pattern of a crystalline rubrene thin film fabricated on an electron-irradiated PS layer. (b) XRD spectra of crystalline rubrene thin films on SiO_2 and irradiated PS, respectively.

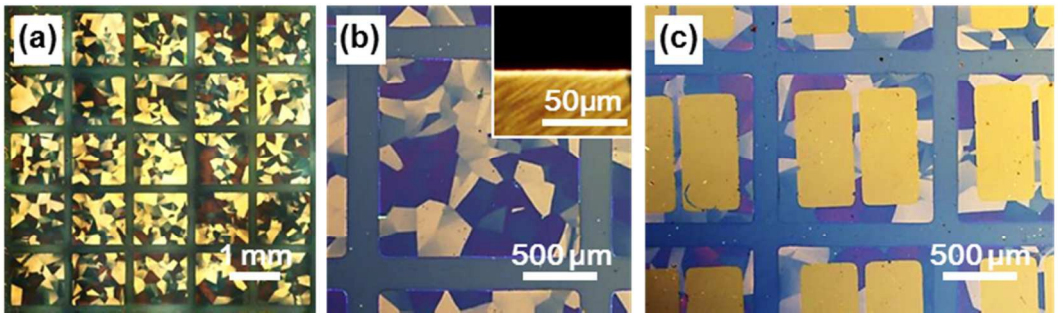

Fig. 4. (a) POM image of a patterned crystalline rubrene thin film. (b) Magnified POM image of a single pattern in (a). Inset shows a boundary of the crystalline rubrene pattern. (c) POM image of fabricated rubrene TFTs with gold electrodes.

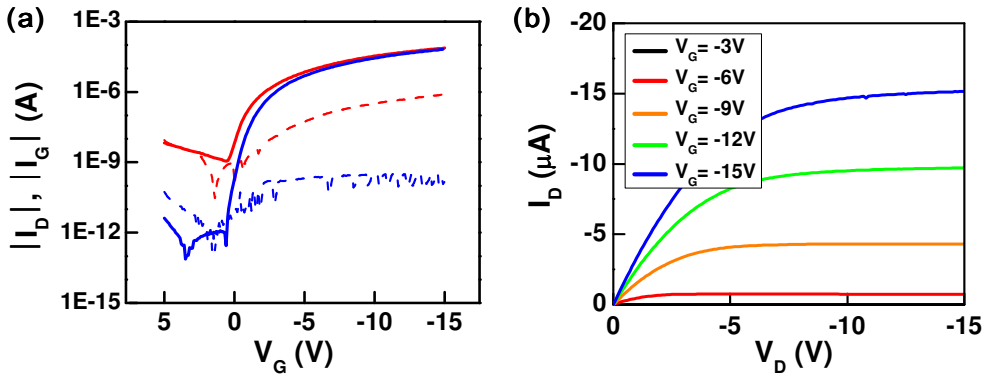

Fig. 5. (a) Typical transfer characteristics of unpatterned (red) and patterned (blue) rubrene thin-film transistors. Solid lines are drain-source currents and dashed lines are gate leakage currents. The transfer curves were measured at a drain-source voltage of -15 V. (b) Typical output characteristics of patterned rubrene thin-film transistors.

	Contact Angle (°)		Surface Energy (mJ m^{-2})		
	Water	Ethylene glycol	γ_s^d	γ_s^p	γ_s
SiO_2	47	31	7.65	46.46	54.11
Irradiated polystyrene	80	61	14.38	11.92	26.30
Crystalline rubrene film	90	59	32.42	1.48	33.90

Table 1. Measured contact angle and surface energy of SiO_2, PS irradiated at the electron fluence of 2×10^{17} cm^{-2}, and a crystalline rubrene film fabricated by the abrupt heating process, respectively. γ_s^d and γ_s^p are dispersion and polar components of the surface energy, respectively. γ_s is the surface energy ($\gamma_s = \gamma_s^d + \gamma_s^p$).

Table of Contents

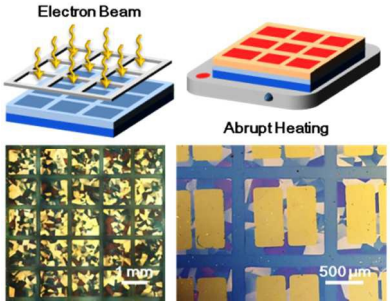

An unprecedented approach to pattern rubrene TFTs is presented by combining an abrupt heating method with selective electron irradiation of polystyrene dielectric layers. The patterned rubrene TFTs exhibited good performances with charge mobilities of ~1.3 $cm^2V^{-1}s^{-1}$ and on/off ratios higher than 10^8.